Biosensors and Bioelectronics 53 (2014) 384–389

Contents lists available at ScienceDirect

Biosensors and Bioelectronics

journal homepage: www.elsevier.com/locate/bios

Novel electrochemical aptamer biosensor based on an enzyme–gold nanoparticle dual label for the ultrasensitive detection of epithelial tumour marker MUC1

Rong Hu, Wei Wen, Qingling Wang, Huayu Xiong, Xiuhua Zhang, Haoshuang Gu, Shengfu Wang *

Hubei Collaborative Innovation Center for Advanced Organic Chemical Materials, Ministry of Education Key Laboratory for the Synthesis and Application of Organic Functional Molecules & College of Chemistry and Chemical Engineering, Hubei University, Wuhan 430062, PR China

ARTICLE INFO

Article history:
Received 28 August 2013
Received in revised form
10 October 2013
Accepted 10 October 2013
Available online 24 October 2013

Keywords:
Aptamer
Biosensor
Gold nanoparticles
Enzyme
MUC1

ABSTRACT

A novel platform based on a hairpin oligonucleotide (HO) switch, gold nanoparticles (AuNPs), and enzyme signal amplification for the ultrasensitive detection of mucin 1 protein (MUC1) was developed in this assay. This HO aptamers and horseradish peroxidase (HRP) were immobilised on the AuNPs to yield HO–AuNP–HRP conjugates. AuNPs were used as labels and bridges between the HO and HRP. HRP was also used as label for catalysing the oxidation of o-phenylenediamine by H_2O_2. The reaction product was 2,3-diaminophenazine (DAP), which was reduced and could be detected at surface of modified electrode. The reduction signal of DAP was used as a probe for the sensitive detection. After the recognition between oligonucleotide and MUC1, biotin was exposed. Biotin, along with the conjugate, was captured by streptavidin onto the surface of modified electrode. Therefore, the detection of target MUC1 which was a membrane-associated glycoprotein of the mucin family could be sensitively transduced via detection of the electrochemical reduction signal of DAP. Compared to other aptasensors, this biosensor has a good linear correlation ranges from 8.8 nM to 353.3 nM and a lower detection limit of 2.2 nM for MUC1. The proposed method provided a new electrochemical approach for the detection of MUC1.

© 2013 Elsevier B.V. All rights reserved.

1. Introduction

Aptamers, which are artificial oligonucleotides in vitro selected through SELEX (systematic evolution of ligands by exponential enrichment) (Roberson and Joyce, 1990; Ellington and Szostak, 1990; Tuerk and Gold, 1990), possess high affinity and high recognition ability for a wide array of targets, including drugs, proteins, carbohydrates, lipids, and other organic or inorganic molecules (Deng et al., 2009; Liu et al., 2013). The most prominent advantage of aptamers is that they can be produced without the need for an animal source and can be synthesised and modified chemically with extreme accuracy at low cost (Gulbakan et al., 2010; Zhou et al., 2011; Li et al., 2013a). Furthermore, aptamers are thermally and chemically stable, are able to undergo several cycles of degeneration/renaturation without losing activity, and show good stability during long-term storage (Nam et al., 2012; Li et al., 2013b). Because of these advantages, aptamers have the potential to be as widely applicable as antibodies in biosensor applications and disease diagnosis.

Mucins are a family of high molecular weight, heavily glycosylated proteins that are bound to cells by an integral transmembrane domain via the formation of a gel matrix (He et al., 2012). The mucin 1 protein (MUC1) is a membrane-associated glycoprotein of the mucin family that contains a hydrophobic membrane-spanning domain of 31 amino acids, a cytoplasmic domain of 69 amino acids, and an extracellular domain consisting of a region of nearly identical repeats of 20 amino acids per repeat (Cheng et al., 2009). MUC1 is the major of mucus layer found on most human epithelia and serves to lubricate and protect surfaces against mechanical damage and chemical and biological insult. MUC1 is also a well-known tumour marker, existing in a variety of malignant tumours (Bossche et al., 2010). It is commonly overexpressed on a broad range of different human epithelia, including breast, gastric, colorectal, lung, prostate, ovarian, pancreatic, and bladder carcinomas (He et al., 2012). Furthermore, the expression of MUC1 in these adenocarcinomatous tissues lacks regular expression patterns, resulting in a ubiquitous, random expression of proteins over the cell surface (Bossche et al., 2010). Therefore, the expression is increased so dramatically that a large amount of MUC1 is found in blood, which makes serum assays for MUC1 potentially useful in tumour detection.

To date, limited studies have been performed with aptamer-based MUC1 detection. The detection method reported by Yu et al. was based on the fluorescence intensity of oligonucleotide-labelled quantum dots by MUC1 peptide (Cheng et al., 2009). Pang et al. performed an assay utilising graphene oxide (GO) as a quencher able

* Corresponding author. Tel.: +86 27 50865309; fax: +86 27 88663043.
E-mail addresses: wangsf@hubu.edu.cn, wangsf8@yahoo.com.cn (S. Wang).

0956-5663/$ - see front matter © 2013 Elsevier B.V. All rights reserved.
http://dx.doi.org/10.1016/j.bios.2013.10.015

to quench the fluorescence of single-stranded dye-labelled MUC1 specific aptamer (He et al., 2012). Liu et al. proposed a strategy for the sensitive detection of MUC1 based on electrochemiluminescence (ECL) resonance energy transfer (ERET) from Bis(2,2′-bipyridine)-(5-aminophenanthroline) ruthenium (II) to GO (Wei et al., 2012). Based on the results of these studies, a novel ultrasensitive electrochemical method for the detection of MUC1 may be more superior.

Our group developed an ultrasensitive electrochemical aptamer biosensor based on an enzyme–gold nanoparticle dual label for the detection of the epithelial tumour marker MUC1 in homogenous solution. Nanomaterials have been widely used in chemical and biological sensing because of their unique optical and mechanical properties (Chen et al., 2012). In this case, multi-walled carbon nanotubes (MWCNTs) were used to modify the electrode and gold nanoparticle (AuNPs) were used as labels and bridges between the hairpin oligonucleotide (HO) and horseradish peroxidase (HRP). HRP has also been used as a label for signal amplification and catalysing the oxidation of o-phenylenediamine (oPD) by H_2O_2 (Zhang et al., 2004; Nam et al., 2004). The oxidation product 2,3-diaminophenazine (DAP) was reduced at −0.56 V at glassy carbon electrode (GCE) and differential pulse voltammetry (DPV) was chosen to detect the enzymatic-generated product (Dobie-Galuska and Wietstock, 1999; Lin and Wheeldon, 2013). A variety of nanomaterials were used to realise multiple signal amplification. As illustrated in Fig. 1, two key components were employed for the aptasensor: a MWCNTs–streptavidin-modified GCE (GCE/MWCNT/streptavidin), which possessed special recognition ability for the enzyme–gold nanoparticle dually labelled aptamers, and dually labelled aptamers, which were designed based on a hairpin with 25 bases in the loop structure complementary to catch the target MUC1. Prior to use, all MUC1 aptamers were heated and then allowed to cool to form hairpin oligonucleotide (HOs). The HO aptamer was modified with thiol at the 5′-end and biotin at the 3′-end. The specific reaction between activated biotin and pre-immobilised streptavidin could realise 4-fold signal amplification because every streptavidin could bind four biotins (Pan et al., 2014). The HO was immobilised on AuNPs by self-assembly via Au–S bonds (Zhang et al., 2010), and the enzyme was immobilised through protein adsorption. Dually labelled aptamers (HO–AuNP–HRP conjugates) were then obtained. In the absence of target MUC1, the immobilised hairpin aptamer was in a "closed" state, which shielded biotin from being captured by the streptavidin. The sensor electrode did not capture the MUC1-unbound conjugate (Fig. 1, state A). In the presence of MUC1, the HO was disrupted, and the biotin was exposed. The biotin, along with the dually labelled aptamers, was then easily captured by the streptavidin-modified electrode (Fig. 1, state B). Then, we transferred the modified electrode into a working solution which contained H_2O_2 and oPD. With nitrogen was continuously fed into the working solution, HRP catalysed the reaction of H_2O_2 oxidising oPD. Therefore, the detection of target MUC1 could be sensitively transduced via detection of the electrochemical reduction signal of DAP (curve b). On the other hand, when the conjugates were not captured on the sensor electrode without MUC1, no catalytic generation of DAP occurred and the very limited background current was observed (curve a).

2. Experimental

2.1. Reagents and materials

All chemicals and solvents were of reagent grade or better. $HAuCl_4$, trisodium citrate, bovine serum albumin (BSA), sodium dodecyl sulphate (SDS), chitosan, HRP, cancer embryo antigen (CEA), myoglobin (MYO), and oPD were purchased from Sigma–Aldrich. Streptavidin was purchased from Promega Corp. Deoxyadenosine triphosphate (dATP) and H_2O_2 were purchased from Aladdin Chemistry Co., Ltd. (Shanghai, China). MUC1 (from the N terminus to the C terminus: PDTRPAPGSTAPPAHGVTS APDTRPAPGSTAPPAHGVTSA) was purchased as a custom synthetic peptide from GL Biochem Co., Ltd. (Shanghai, China). MWCNTs were purchased from Chengdu Organic Chemicals Co., Ltd. (Chengdu, China). Thiol-labelled MUC1 aptamers (5′-HS-$(CH_2)_6$-ACA CGG CAG TTG ATC CTT TGG ATA CCC TGG CGT GT-biotin-3′) were acquired from Sangon Biological Engineering Technology & Services Co., Ltd. (Shanghai, China). The supporting electrolyte was 0.1 mol L^{-1} phosphate buffer solution (PBS) prepared with Na_2HPO_4 and KH_2PO_4 and the pH was adjusted with NaOH or H_3PO_4. And the red precipitate was dispersed

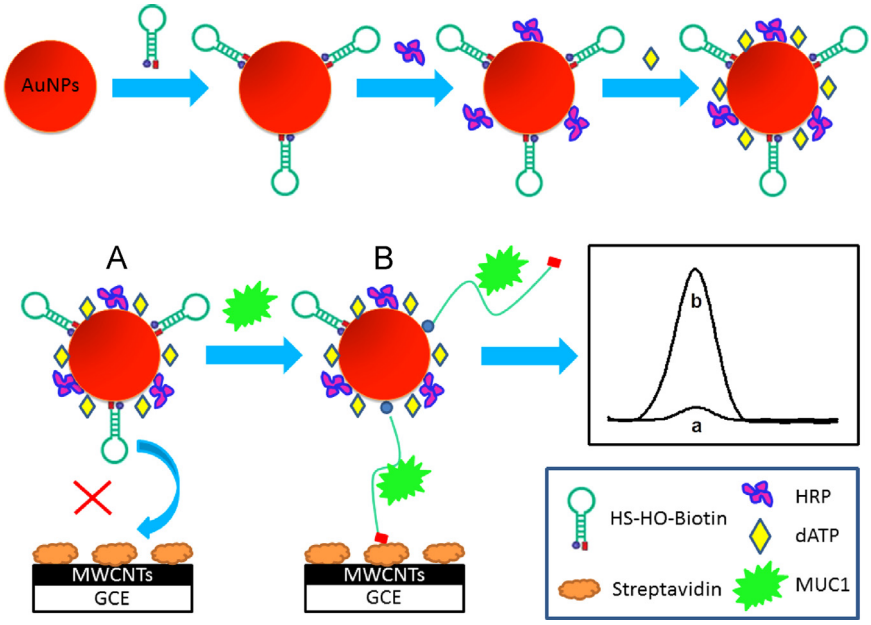

Fig. 1. Schematic diagram about MUC1 detection with the HO switch. (A) In the absence of MUC1, the biotin is shielded and thus inaccessible to the streptavidin. Then, a very limited background current (inset) was observed (curve a). (B) Upon target binding, the disruption of the stem-loop makes the biotin exposed. And then the biotin, along with the dually labelled aptamers, is easily captured by the streptavidin-modified electrode (curve b).

in phosphate-buffer (0.01 M PBS, containing 5 mM $MgCl_2$, pH 7.4) solution. The Tris–HCl buffer used in this experiment consisted of 20 mM Tris–HCl (pH 7.4), 100 mM NaCl and 5 mM $MgCl_2$. All solutions were prepared with doubly distilled water.

2.2. Apparatus

Electrochemical measurements were carried out with a model CHI660C electrochemical analyser (CH Instrumental Co., USA) controlled by a personal computer. A three-electrode system was used in the measurements, with a glassy carbon electrode (GCE, 3 mm in diameter) as the working electrode, a saturated calomel electrode (SCE) as the reference electrode, and a platinum wire as the auxiliary electrode. The pH value of the solutions was determined using a 320-S acidity metre (Mettler-Toledo, Switzerland). Branson 2000 ultrasonic cleaner (USA) was used to clean the electrodes.

2.3. Preparation of HO–AuNP–HRP conjugates

The AuNPs were prepared according to previously reported procedures with slight modification (Grabar et al., 1995; Fan et al., 2010). All glassware used in this preparation was thoroughly cleaned in aqua regia (3 parts HCl and 1 part HNO_3), rinsed in doubly distilled water, and oven-dried prior to use. Caution: aqua regia is extremely dangerous and should be handled with extreme caution. Gloves and eye protection are required for handing (Liu et al., 2011). In brief, in a 500 mL round-bottom flask, 100 mL of 0.01% $HAuCl_4$ solution was boiled with vigorous stirring, followed by the addition of 2.7 mL of 1% trisodium citrate. The solution turned deep blue within 20 s, and the final colour, wine-red, appeared after 60 s. Boiling was pursued for an additional 10 min, after that the heating source was removed and the colloid solution was stirred for another 10 min. The obtained AuNPs were then stored in a brown glass bottle at 4 °C and used to prepare the HO–AuNP–HRP conjugates. The resulting AuNPs solution was imaged by transmission electron microscope (TEM).

Prior to use, all the MUC1 aptamers were heated to 95 °C for 2 min and then allowed to cool to room temperature over 12 h, after which, all the MUC1 aptamers could form HOs (Chen et al., 2012). The HOs were immobilised on AuNPs by self-assembly as follows: 100 μL of HO buffer (100 μM HO dissolved in Tris–HCl buffer) was added to 1 mL of AuNP solution. After shaking for 90 min at room temperature (RT), 30 μL of 4 mg/mL HRP was added to the solution and shaken for 30 min at RT. Then, 40 μL of 14.1 μM dATP was added to the solution and shaken for 30 min. The HO–AuNP–HRP conjugates were then incubated at 4 °C for 6 h to increase the stability. The conjugates were removed by centrifugation for 12 min at 12,000 rpm, followed by the removal of the supernatant. The precipitate was then washed twice with 0.01 M PBSB (PBS pH 7.4, 1% BSA), dispersed in 1 mL of 0.01 M PBS (pH 7.4), and stored at 4 °C for further use (He et al., 2010a).

2.4. Preparation of the GCE–MWCNT–chitosan/streptavidin

First, a GCE was carefully polished on chamois leather with slurries of alumina of 0.3 and 0.05 μm to create a mirror finish and then sonicated with absolute ethanol and double-distilled water, respectively. The cleaned GCE was allowed to dry at room temperature. Before the modification of the GCE, 1.5 mg of the purified MWCNTs (0.5 mg/mL) was dispersed into 3.0 mL of 5 mM SDS by ultrasonic agitation for 40 min to yield a homogeneous MWCNT suspension. Then, 1 mL of 1% chitosan was mixed with 1 mL of 2 mg/mL streptavidin dissolved in PBS (0.1 M, pH 7.0). A cleaned GCE was coated with 7.0 μL of the MWCNT suspension and dried in air for 2 h. Next, 5.0 μL of mixed solution containing 1 mg/mL streptavidin and 0.5% chitosan was dropped onto the surface of the GCE/MWCNTs and dried at room temperature to remove the solvent.

2.5. Procedures

10 μL MUC1 was added to 50 μL of the HO–AuNP–HRP conjugates, followed by 2 h of incubation at 37 °C. The modified electrode (GCE/MWCNT/streptavidin) was then incubated in the mixing solution for an additional 20 min. When the incubation was complete, the resulting electrode was gently rinsed before electrochemical characterisation.

All measurements were conducted in PBS (0.1 M, pH 7.0) solution. Before the measurements, nitrogen was continuously fed into 5.0 mL of PBS (0.1 M, pH 7.0) for 15 min to remove oxygen. After adding 100 μL of 100 mM oPD, nitrogen was passed through the solution for an additional 10 min. Next, 5 μL of 30% H_2O_2 was added. We measured the DPV immediately after the H_2O_2 addition. The DPV experiment was performed from −0.2 V to −0.8 V with a pulse amplitude of 50 mV and a pulse width of 50 ms. During the potential scanning, a distinct electrochemical signal was obtained at −0.56 V, which was used for the identification and quantification of MUC1. The DPV was measured once a minute until the peak current achieved balance.

3. Results and discussion

3.1. Morphology studies by SEM and TEM

We characterised the morphology by SEM and TEM. As shown in Fig. 2A, typical TEM images of AuNPs indicated that they have a diameter of approximately 12–15 nm and a narrow size distribution. The SEM morphologies of MWCNTs and MWCNT–chitosan/streptavidin protein hybrid films were shown in Fig. 2 (B and C, respectively). It was obvious from the images that the MWCNTs distributed onto the surface of the GCE and formed a three-dimensional network structure, which enabled the GCE/MWCNTs to have a much higher specific area (Fig. 2B). As shown in Fig. 2C, the SEM images indicated that the streptavidin was embedded in the void in the MWCNTs assembly, which was attributed to the high viscosity of chitosan. And the immobilised MWCNT–chitosan/streptavidin protein hybrid films provided recognition between streptavidin and biotin.

3.2. Electrochemical impedance spectroscopy (EIS) and cyclic voltammetry (CV) behaviours of GCE

To understand the characterisation of the modified electrode, the electrochemical behaviours of GCE under different conditions were studied by EIS and CV. As show in Fig. S1A, an obvious redox peak was observed by the bare GCE (Fig. S1A, curve a). And the CV response was enhanced after the adsorption of MWCNTs on the electrode (Fig. S1A, curve b). With the formation of streptavidin proteins and chitosan hybrid films, the electrode showed remarkable blocking owing to their non-electroactive property that obstructs electron transfer (Fig. S1A, curve c). In the presence of 100 nM MUC1, the CV response was strongly enhanced (Fig. S1A, curve d) due to AuNPs enhancing electron transfer and steric hindrance effect of HRP–AuNPs dually labelled aptamers. The impedance spectra under different conditions were also investigated. In Fig. S1B, the bare GCE and MWCNT/GCE produced a very small resistance (Fig. S1B, curves a and b). Resistance increased dramatically with the modification of streptavidin (Fig. S1B, curve c). However, the semicircle domain decreased (Fig. S1B, curve d) upon the addition of target MUC1 and HO–AuNP–HRP conjugates, which

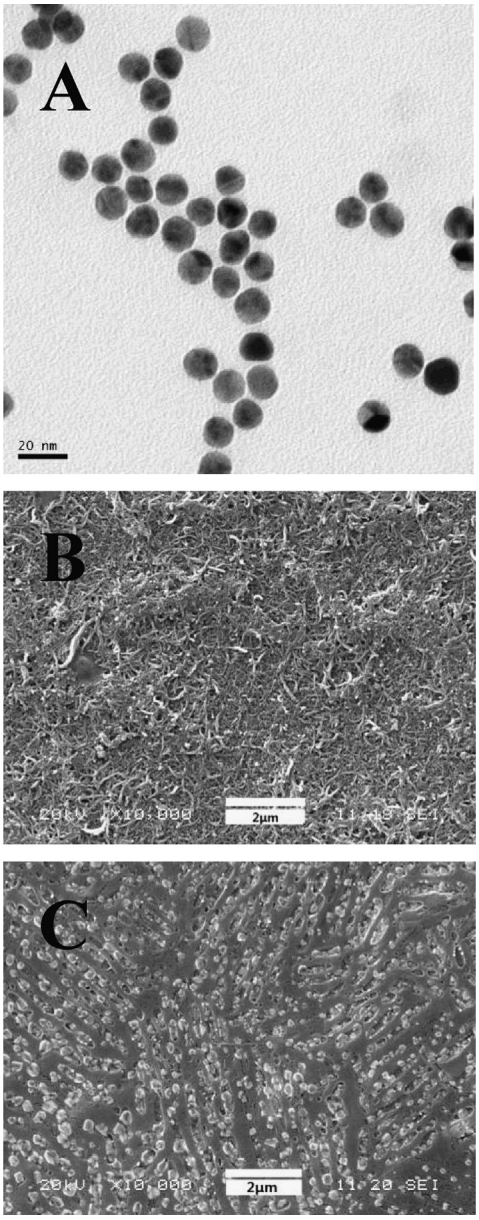

Fig. 2. TEM image of (A) AuNPs. SEM images of (B) MWCNTs and (c) MWCNTs–chitosan/streptavidin.

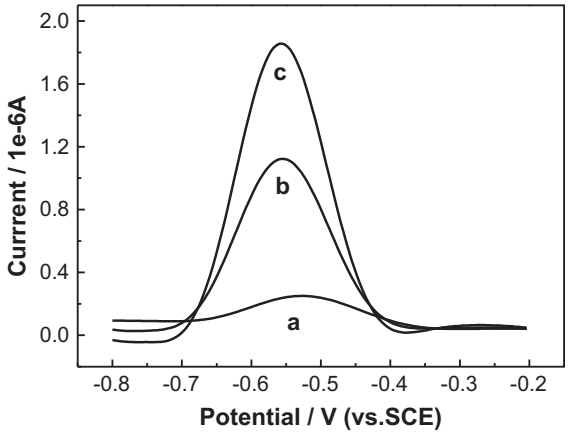

Fig. 3. The DPV responses of the HO–AuNP–HRP with MUC1 target at the concentrations of: (a) 0 nM at GCE–MWCNT–chitosan/streptavidin, (b) 120 nM at GCE–chitosan/streptavidin, and (c) 120 nM at GCE–MWCNT–chitosan/streptavidin.

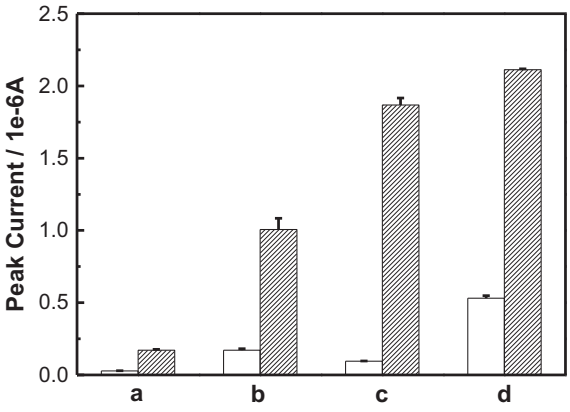

Fig. 4. The DPV response of 10 μM HO probe with different concentrations of HRP was obtained in PBS 7.0 in the case of no MUC1 (left) and 150 nM MUC1 (right). The added HRP: (a) 10 μL, (b) 15 μL, (c) 30 μL, and (d) 50 μL. Error bars are obtained based on three independent measurements.

greatly enhanced the electron transfer in accordance with CV response.

3.3. Verification of the design principle

To verify the feasibility of the designed homogenous electrochemical amplified strategy for MUC1 detection, differential pulse voltammograms (DPV) were obtained in the presence of MUC1 and in control experiments. In the experiment, 30 μL of HO–AuNP–HRP conjugates were incubated with target MUC1. As shown in Fig. 3, a very low background DPV signal was observed (curve a) in the absence of MUC1. While in the presence of MUC1 target, the DPV signal was detected by the chitosan/streptavidin hybrid film modified electrode (curve b) and further enhanced DPV signal was detected by the MWCNT–chitosan/streptavidin hybrid film modified electrode (curve c). The experimental results showed that the MWCNTs could increase the effective area of the electrode and significantly increase peak currents. The results also indicated that MUC1 was detected based on the enzyme–AuNPs dually label aptamer.

3.4. Optimisation of the immobilisation procedure of HRP and HO on the AuNPs surface

The general approach to immobilising HRP and thiolated HO onto AuNPs is through protein adsorption and self-assembly via Au–S bonds. The immobilisation of HRP and thiolated HO onto AuNPs is the most important step in preparing ultrasensitive electrochemical aptasensors (He et al., 2010b). The amounts of HRP and thiolated HO affect the catalytic efficiency of the enzyme. We studied the effect of the HO and HRP amounts based on the signal-to-background (S/B) ratio of the tests. In Fig. 4, the effect of the HRP concentration for the conjugate preparation was shown at the constant HO concentration. When 10, 15, 30, and 50 μL of HRP were added, the S/B ratio was 6.2, 5.9, 19.7, and 4.0, respectively. The highest S/B ratio was obtained with adding 30 μL of HRP (Fig. 4c). The variation in S/B ratio may be due to the steric hindrance effect of HRP and competition between HRP and HO. The adsorption of less HRP on the AuNPs resulted in decreasing the amounts of catalytic generation of DAP (Fig. 4a and b). And more HRP on the AuNPs resulted in huge background and less HO–AuNP–HRP Conjugates captured on the electrode. Large amount of HRP adsorbed meant huge background even though very low

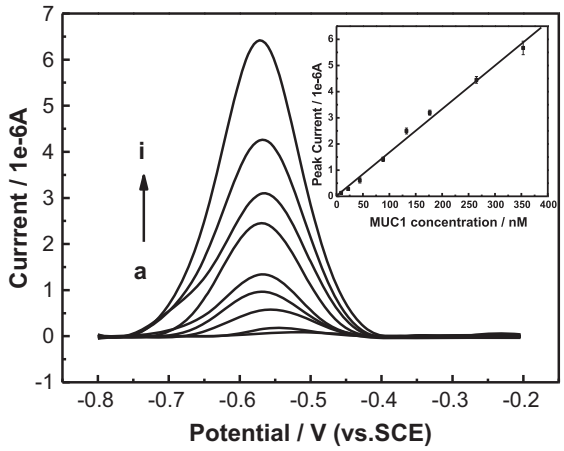

Fig. 5. DPV responses for detection of different concentrations of target MUC1: (a) 0 M, (b) 8.8 nM, (c) 22.1 nM, (d) 44.2 nM, (e) 88.3 nM, (f) 132.5 nM, (g) 176.7 nM, (h) 265 nM, and (i) 353.3 nM. Inset: calibration curve corresponding to the DPV peak current for variable concentrations of MUC1. Error bars are obtained based on three independent measurements.

amount of the conjugate captured on the sensor electrode (Fig. 4d).

3.5. Optimisation of the incubation time between biotin and streptavidin

There are two steps in the recognition process: recognition between aptamer and MUC1, which was finished in advance by mixing target MUC1 and HO–AuNP–HRP conjugates, and recognition between biotin and streptavidin. We got the incubation time between aptamer and MUC1 from references (He et al., 2012). After the recognition between oligonucleotide and MUC1, biotin was exposed. Biotin, along with the conjugate, was captured by streptavidin onto the surface of modified electrode. The incubation time between biotin and streptavidin would affect the amount of conjugate captured to the surface of modified electrode. The impact of the incubation time between biotin and streptavidin was investigated (Fig. S2). The electrode (GCE–MWCNT–streptavidin) was incubated in the mixed solution that includes target MUC1 and the conjugate for 0, 5, 10, 15, 20, 30, and 45 min. The current increased with the incubation time and almost saturated within 20 min. We concluded that the incubation time of 20 min was optimal.

3.6. Calibration curve and application of the aptamer biosensor

The sensitivity of the aptasensor was investigated by DPV measurements. Fig. 5 revealed a good linear relationship between the DPV peak currents and the MUC1 concentration from 8.8 nM to 353.3 nM. This biosensor is superior in sensitivity, with a wide linear range of three orders of magnitude ($R^2=0.9962$). The detection limit (LOD) is estimated to be 2.2 nM ($3S_0$, in which S_0 is the standard deviation for the blank solution), which is lower than those of a reported aptamer-antibody hybrid sandwich ELISA sensor, quantum-dot-based fluorescence readout sensor (Cheng et al., 2009), and GO-based fluorescent aptasensor (He et al., 2012).

Furthermore, we applied this aptasensor to the detection of the target MUC1 in human serum, which is one of the most challenging media, containing many complex components. For serum spiked with MUC1 at different levels, the recoveries ranged from 101.2% to 108.9%. These results clearly indicated that the proposed aptasensor can be used to detect MUC1 in practical samples with good sensitivity.

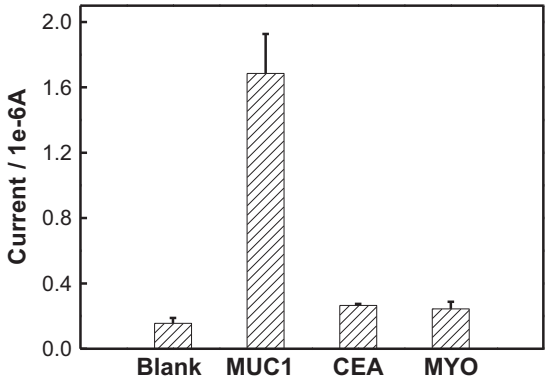

Fig. 6. Selectivity of the proposed electrochemical aptamer sensor to MUC1, CEA, and MYO at 200 ng/mL, respectively. Error bars are obtained based on three independent measurements.

3.7. The selectivity of the biosensor

To evaluate the selectivity of the MUC1 aptasensor, a control experiment using CEA and MYO as samples was performed. In a typical experiment, the aptasensor was incubated with 200 ng/mL CEA, 200 ng/mL MYO, and 200 ng/mL MUC1 in PBS (0.1 M, pH 7.0) in separate trials. As shown in Fig. 6, a significant DPV signal was observed for MUC1, which was much higher than that for CEA and MYO.

4. Conclusions

In conclusion, our group developed a multiple signal amplification strategy for ultrasensitive detection of epithelial tumour marker MUC1 based on HO-functionalized AuNPs amplification coupled with enzyme-linkage reactions. This strategy was achieved by MWCNTs to modify biosensor surface for accelerating electron transfer, and AuNPs carried HO and enzyme as tracing tag for electrochemical detection. Compared to other aptasensors, this approach enables rapid detection with high specificity, low limit of detection, and wide linear range. In the future, we plan to replace AuNPs with gold nanorods (GNRs) to get a lower limit of detection because GNRs can raise the immobilised enzyme activity. The proposed method provided a new electrochemical approach for the detection of MUC1. It also shows great promise for point-of-care diagnosis of genetic diseases and for the detection of cancer.

Acknowledgements

This work was supported by the National Natural Science Foundation of China (nos. 21175032 and 51173038), the Ph.D. Programs Foundation of Ministry of Education of China (no. 20114208130001), and the Natural Science Fund for Creative Research Groups of Hubei Province of China (no. 2011CDA111).

Appendix A. Supplementary material

Supplementary data associated with this article can be found in the online version at http://dx.doi.org/10.1016/j.bios.2013.10.015.

References

Bossche, J.V., Al-Jamal, W.T., Tian, B., Nunes, A., Fabbro, C., Bianco, A., Prato, M., Kostarelos, K., 2010. Chem. Commun. 46, 7379–7381.
Chen, X., Hong, C.Y., Lin, Y.H., Chen, J.H., Chen, G.N., 2012. Anal. Chem. 84, 8277–8283.

Chen, Y., Xu, J., Su, J., Xiang, Y., Yuan, R., Chai, Y.Q., 2012. Anal. Chem. 84 (18), 7750–7755.
Cheng, A.K.H., Su, H.P., Wang, Y.A., Yu, H.Z., 2009. Anal. Chem. 81, 6130–6139.
Deng, C.Y., Chen, J.H., Nie, L.H., Nie, Z., Yao, S.Z, 2009. Anal. Chem. 81, 9972–9978.
Dobie-Galuska, A.A., Wietstock, S.M., 1999. J. Chem. Educ. 76, 642–644.
Ellington, A.D., Szostak, J.W., 1990. Nature 346, 818–822.
Fan, H., Xu, Y., Chang, Z., Xing, R., Wang, Q.J., He, P.G., Fang, Y.Z., 2010. Biosens. Bioelectron. 26, 2655–2659.
Grabar, K.C., Freeman, R.G., Hommerm, M.B., Natan, M.J., 1995. Anal. Chem. 67, 735–743.
Gulbakan, B., Yasun, E., Shukoor, M.L., Zhu, Z., You, M.X., Tan, X.H., Sanchez, H., Powell, D.H., Dai, H.J., Tan, W.H., 2010. J. Am. Chem. Soc. 132, 17408–17410.
He, Y., Lin, Y., Tang, H.W., Pang, D.W., 2012. Nanoscale 4, 2054–2059.
He, Y.Q., Zeng, K., Gurung, A., Baloda, M., Xu, H., Zhang, X.B., Liu, G.D., 2010a. Anal. Chem. 82, 7169–7177.
He, Y.Q., Zhang, S.Q., Zhang, X.B., Baloda, M., Gurung, A.S., Xu, H., Zhang, X.J., Liu, G.D., 2010b. Biosens. Bioelectron. 26, 2018–2024.
Li, F., Du, Z.F., Yang, L.M., Tang, B., 2013a. Biosens. Bioelectron. 41, 907–910.
Li, F., Yang, L.M., Chen, M.Q., Qian, Y., Tang, B., 2013b. Biosens. Bioelectron. 41, 903–906.
Liu, S.N., Wu, P., Li, W., Zhang, H., Cai, C.X., 2011. Anal. Chem. 83, 4752–4758.
Liu, S.F., Wang, Y., Zhang, C.X., Lin, Y., Li, F., 2013. Chem. Commun. 49, 2335–2337.
Lin, J.L., Wheeldon, I., 2013. ACS Catal. 3, 560–564.
Nam, E.J., Kim, E.J., Wark, A.W., Rho, S., Kim, H., Lee, H.J., 2012. Analyst 137, 2011–2016.
Nam, J., Stoeva, S.I., Mirkin, C.A., 2004. J. Am. Chem. Soc. 126, 5932–5933.
Pan, Y.L., Shan, W.Q., Fang, H.T., Guo, M.L., Nie, Z., Huang, Y., Yao, S.Z., 2014. Biosens. Bioelectron. 52, 62–68.
Roberson, D.L., Joyce, G.F., 1990. Nature 344, 467–468.
Tuerk, C., Gold, L., 1990. Science 249, 505–510.
Wei, W., Li, D.F., Pan, X.H., Liu, S.Q., 2012. Analyst 137, 2101–2106.
Zhang, Y.Y., Tang, Z.W., Wang, J., Wu, H., Maham, A., Lin, Y.H., 2010. Anal. Chem. 82, 6440–6446.
Zhang, Y., Pothukuchy, A., Shin, W., Kim, Y., Heller, A., 2004. Anal. Chem. 76, 4093–4097.
Zhou, Z.X., Du, Y., Dong, S.J., 2011. Anal. Chem. 83, 5122–5127.